Application of PIV/LIF and Shadow-Image to a Bubble Rising in a Linear Shear Flow Field

by

Akiko FUJIWARA*, Akira TOKUHIRO**, and Koichi HISHIDA*

* Department of System Design Engineering, Keio University,
3-14-1 Hiyoshi, Kohoku-ku, Yokohama, 223-8522 JAPAN
** Japan Nuclear Cycle Development Institute, 4002 Narita, Oarai-machi, Ibaraki-ken, 311-1393 JAPAN

ABSTRACT

In the present study, the objective is to obtain fundamental knowledge of the influence of the lift force on the bubble and its motion induced by the surrounding flow field. We explored the flow structure in the vicinity of the bubble and also deformation of the bubble shape respectively by PIV/LIF and a projecting technique. As our system, we chose a large single air bubble with an equivalent bubble diameter (D_e) 8mm, in a vertical shear flow. Velocity measurements were made using one digital high-speed CCD camera for Digital Particle Image Velocimetry (DPIV) with fluorescent tracer particles. The recorded image data are analyzed by cross-correlational technique. A second CCD camera was used to detect the bubble's shape and translational motion via backlighting from a square array of infrared LED's. Figure 1 shows the time series of the velocity vector field and vorticity contours around the bubble. We confirmed that the shear rate acts on the ellipsoidal bubble as a lift force, which induces bubble motion toward a direction where the relative velocity decreases. We clarified that bubble trajectory was influenced vorticity which leaved from bubble edges quantitatively by measured the vorticity in the vicinity of bubble.

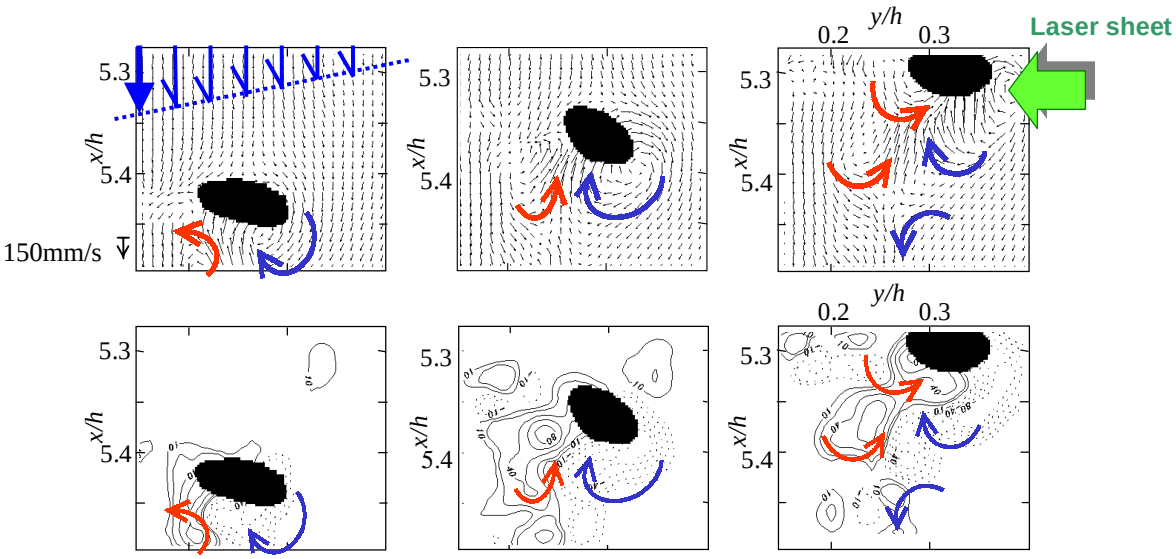

Fig. 1. Time series of flow structure around the bubble.
Instantaneous velocity vector fields (Upper).
Instantaneous vorticity contours (Lower). Line: positive, doted: negative.

1. INTRODUCTION

The study of flow around a solid body such as a hemisphere or that around a single rising gas bubble in a volume of liquid is classic example of problems in fluid mechanics of single- and multi-phase flows. It goes without saying that from an understanding of such rudimentary systems, one often extrapolates this knowledge, for better or worse, to larger systems such as fluidized-beds, bio-reactor bubble columns and other equipment involving solid-liquid, gas-liquid and even solid-gas-liquid flows. Our base of knowledge on the fundamental aspects of bubbles, drops and particles accumulated over many years are contained in such texts as those by Levich (1962) and Clift et al. (1978).

Recently various calculation techniques and simulation models of dispersed phase in gas-liquid two-phase flow are proposed with a development of computer performance (Tomiyama, 1998, Bunner and Tryggvason, 1999, Hao and Prosperetti, 1999). And these are getting much popular to predict the behavior of certain particular types of flows. Nevertheless it is not clarified enough that the correlation between the macroscopic flow structure and microscopic influence of interaction between dispersed bubble and surrounding liquid phase, thus we are confronted with some problems to apply such technique or models to other situations. And we need to elucidate the microscopic interaction between gas and liquid phases experimentally. One of the significant challenges in proper modeling of gas-liquid two-phase flow is the clarification of the interaction amongst various time- and length-scales describing the flow. Recently many measurement systems with image processing technique have developed and they were applied to bubbly flow (Fan and Tsuchiya, 1990, Brücker, 1998). We (Tokuhiro et. al., 1998, Tokuhiro et. al., 1999) have developed a particular technique to investigate the flow around and in the wake region of a single bubble and two similar sized air bubble confined in a downward flow of water. Of particular interest is the localized phenomena, such as the factors influencing the lift force on the bubble; that is, the interaction between gas/liquid phases and the associated transfer mechanisms.

In the present study, the objective is to obtain fundamental knowledge of the influence of the lift force on the bubble and its motion induced by the surrounding flow field. We explored the flow structure in the vicinity of the bubble and also deformation of the bubble shape respectively by DPIV applied LIF technique as fluorescent tracer particles and a shadow-image technique. We estimated the lift force on the bubble, bubble trajectory, subsequent deformation, and the interactive influence on flow structure.

2. MEASUREMENT METHOD

2.1 Measurement Method for Flow Structure around the Bubble

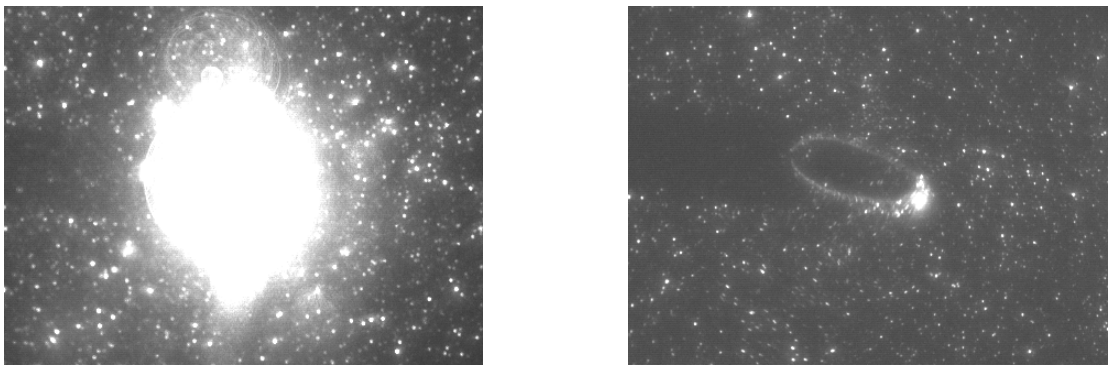

a) *b)*

Fig. 2. Typical snapshot of particle image around the bubble.
a) High intensity of light reflection from bubble's surface.
b) Fluorescent tracer particles image in the vicinity of bubble.

In order to measure the flow structure around the bubble, specifically to detect the interaction between the bubble motion and the flow field which it encounters, we implemented a Digital Particle Image Velocimetry (DPIV) system previously described by Sakakibara et al. (1993 a and b) and Tokuhiro et al. (1998). The diameter of the bubble that we measured was approximately 1000 times larger than that of tracer particles. From initial trials we noticed that the intensity of light reflected from the bubble's surface saturated the CCD device so that the intensity of light from the tracer particles was overwhelmed. And we cannot detect the tracer images in the vicinity of the bubble as shown in Figure 2 a). Thus we applied Laser Induced Fluorescence (LIF) as fluorescent tracer particles. Methyl methacrylate ($H_2C=C(CH_3)COOCH_3$) with Rhodamine-B as the fluorescence dye polymerizes to give particle. We could detect fluorescence emitted by the particles through a color filter to cut the reflection into a CCD camera as shown in Figure 2 b). The diameter of the tracer particles is approximately 1~10 μm and a specific density is 1.02. With this set-up we could measure the flow structure in the vicinity of the bubble. In this system, image data are analyzed by cross-correlational technique, so that we can obtain the velocity vector at each location.

2.2 Measurement Method for Detection of the Bubble Shape and Trajectory

Next in order to capture the bubble's shape and motion simultaneously we supplemented the DPIV-LIF system with a projection technique using infrared LEDs as the light source specifically prepared for this experiment. Figure 3 shows a bubble's image as illuminated from the back side, and imposed on a grayscale background. The bubble has been captured at one instant of a continuous oscillatory motion. The emitted light passed through a filter attached to the CCD camera and recorded the shadow and the infrared-light.

Figure 4 depicts our arrangement consisting of two CCD cameras; one for DPIV-LIF (left camera in Figure 4) and the other (right) for detecting bubble shape. A square "window" array of infrared LEDs permitted a view for DPIV-LIF. In order to capture both the bubble shape and flow field simultaneously, we synchronized the triggering of the laser, the LEDs and the two CCD cameras.

3. EXPERIMENTAL APPARATUS AND EXPERIMENTAL CONDITIONS

As for the experimental apparatus it consisted of two rectangular tanks, a lower and upper, and vertical, square

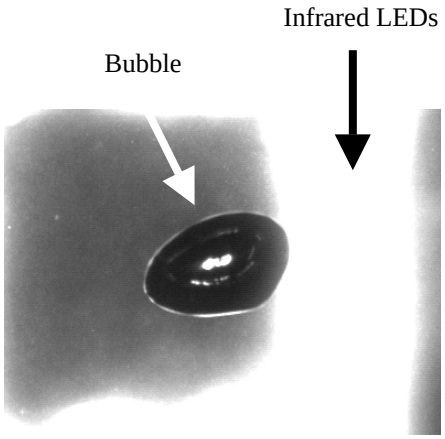

Fig. 3. Typical snapshot of bubble shadow image.

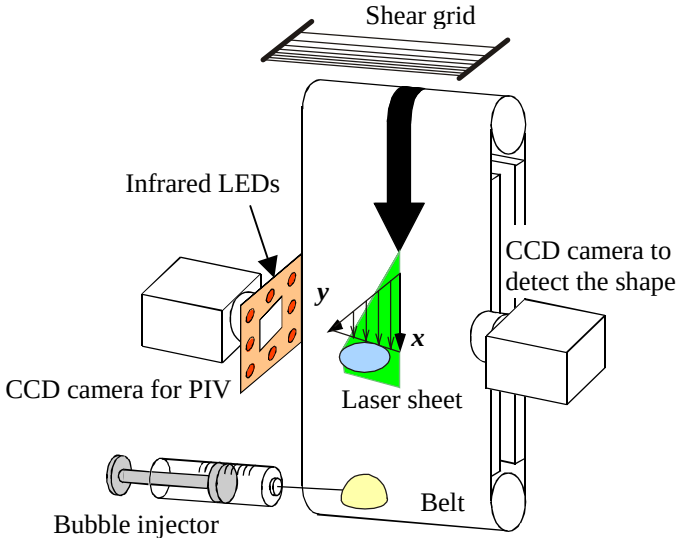

Fig. 4. Schematic of measurement setup.

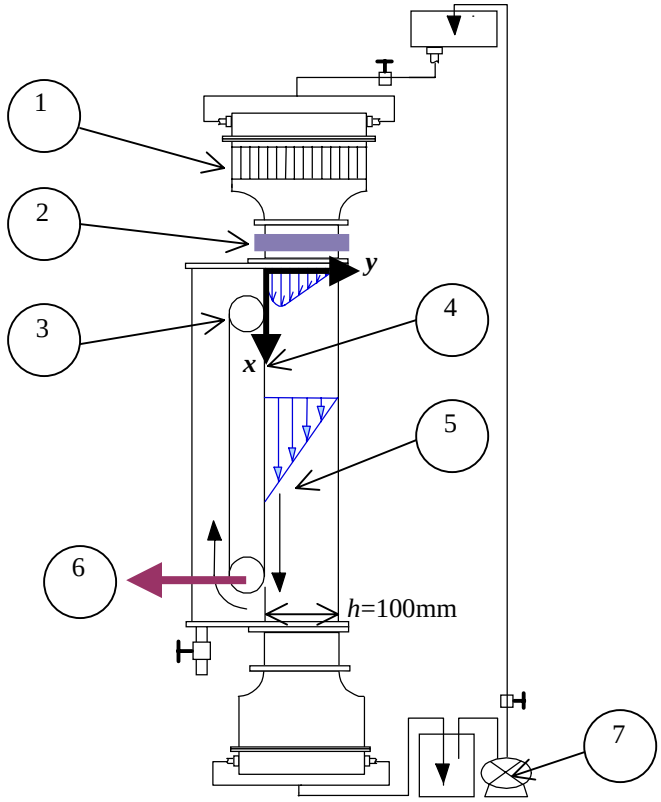

1. Honeycomb
2. Shear grid
3. Pulley
4. Belt
5. Test section
6. Motor
7. Pump

Fig. 5. Schematic of experimental apparatus.

acrylic channel. A schematic is shown in Figure 5. In the middle of channel there is a looped belt connected to a variable speed so that we can induce a vertical shear flow between belt and the wall. We defined the region with downward flow as the test section which is 100x100mm^2 cross section area, and approximately 1000mm in length. The fluid was pumped back up to the upper tank and circulated in a manner to minimize secondary flow. At the top of the channel there is an entrance section with a honeycomb used to rectify the incoming flow. In order to tailor a stable linear shear flow we set up a grid to induced the desired shear rate. We defined the middle of the channel in span direction on the belt as the origin, downward flow direction as x-axis, and cross-sectional direction as y-axis. The laser sheet entered at z/h = 0 and illuminated a x-y plane.

Table 1 shows the experimental conditions. We used tap water and 16-weight % glycerin water solution (16w% GWS) as working fluid. 16w% GWS has approximately 1.5 times the viscosity of tap water. The average shear rate k_{avg} were –0.5 when the fluid was tap water, while –2.3 when it was 16w% GWS. The equivalent bubble diameter D_e=8mm and corresponding dimensionless numbers were defined as below, (1) to (4). In equation (1) bubble relative velocity U_{rel} was estimated from experimental data.

$$Re_{rel} = \frac{D_e U_{rel}}{\nu}, U_{rel} = U_{bubble} - U_{fluid} \quad (1)$$

$$Re_k = \frac{D_e^2 k_{avg}}{\nu} \quad (2)$$

$$Eo = \frac{g D_e^2 \rho_l}{\sigma} \quad (3)$$

$$M = \frac{g \mu_l^4}{\rho_l \sigma^3} \quad (4)$$

Table 1. Experimental conditions

D_e[mm]	k_{avg}[s^{-1}]	Re_{rel}	Re_k	Eo	M
8 (tap water)	-0.5	1820~1900	32.6	8.4	2.25×10^{-11}
8 (16w%GWS)	-2.3	1330~1410	110.2	10.0	1.25×10^{-10}

4. RESULTS AND DISCUSSIONS

Figure 6 shows the flow structure in single phase (liquid) at each condition. We confirmed that the flow is nearly linear shear flow in the observed area. The maximum u_{rms} measured by LDV is approximately 10%. The velocities V (average velocity in y direction) and W (average velocity in z direction) can be neglected (approximately 0). We can thus regard the flow structure as being approximately two-dimensional linear shear flow.

The bubble ascended in the flow field as shown in Figure 6. Figure 7 and 8 show the flow structure around the bubble indicated by velocity vector field and vorticity color contours in time series. Each picture depicts the instantaneous flow structure. Vorticity is defined in terms of that circulation and calculated using equation (5),

$$\omega_{0,0} \equiv (-u_{1,1}\Delta x - u_{0,1}\Delta x - v_{-1,1}\Delta y - v_{-1,0}\Delta y + u_{-1,-1}\Delta x + u_{0,-1}\Delta x + v_{1,-1}\Delta y + v_{1,0}\Delta y)/(4\Delta x\Delta y) \quad (5)$$

Where Δx and Δy are the distance between each point of data in x, y direction. The sampling rate was approximately 23.5ms based on a limited framing rate of the CCD camera (maximum frame rate is 85 fps). In Figure 7 we used tap water, while in Figure 8, 16w% GWS. Under both conditions a vortex grew at the edge of the bubble where the shear rate was high and shed from the bubble's edge. In Figure 8 in particular the vorticity at the right exhibits relatively higher values than the left as the bubble orients itself toward the right (from t=0sec to 70.5msec). When the relative vorticity reaches–100s^{-1}, the vortex is shed and the bubble reorients itself (at t=94.0msec). In both Figs. 7 and 8 maximum positive and negative vorticies are approximately ±100s^{-1}. These vorticies appear turbulent in nature. We confirmed this sequence of events in many experiment cases.

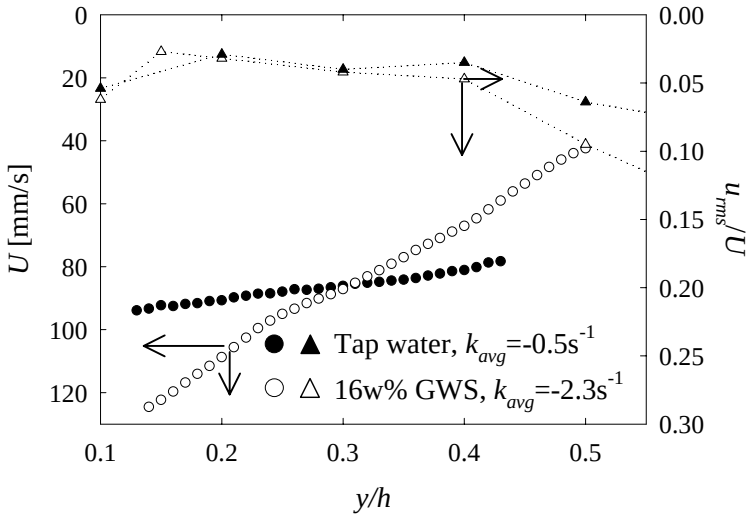

Fig. 6. Flow structure in single phase.

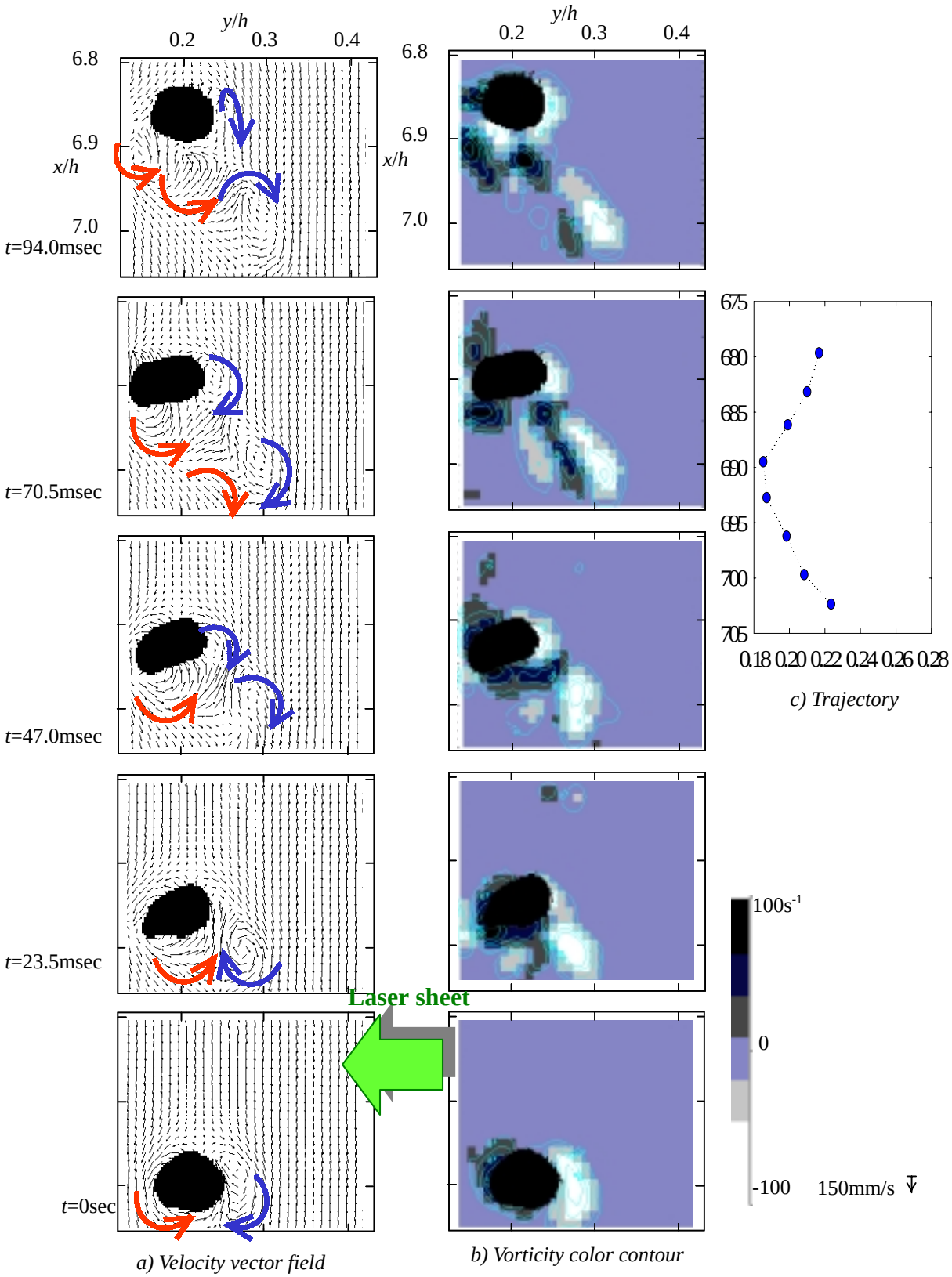

Fig. 7. Flow structure around the bubble in tap waster.
(k_{avg}=-0.5s^{-1}, Re_{rel}=1820~1900, Eo=8.4, M=2.25x10^{-11})

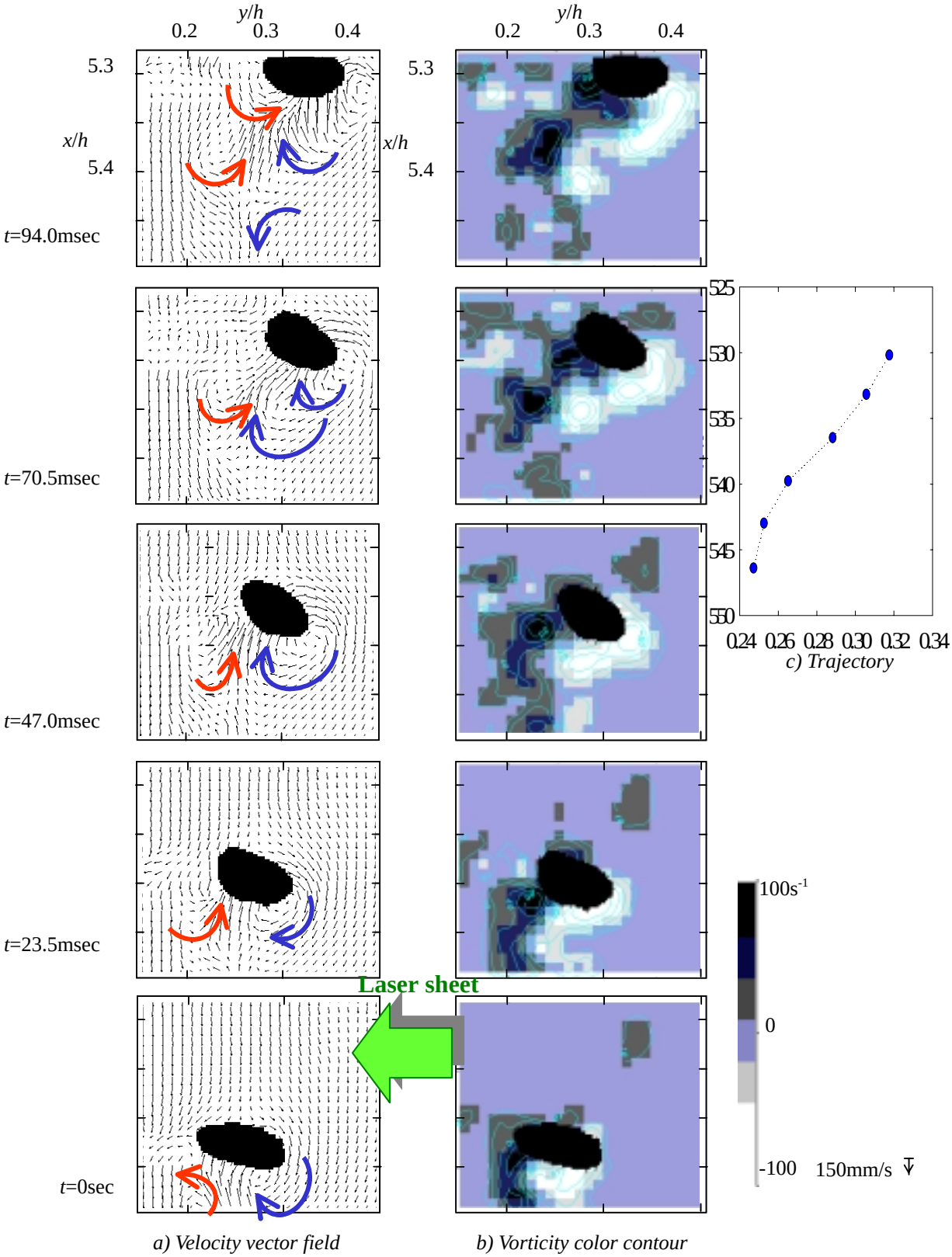

Fig. 8. Flow structure around the bubble in 16w% GWS.
(k_{avg}=-2.3s^{-1}, Re_{rel}=1330~1410, Eo=10.0, M=1.25x10^{-10})

We showed the bubble trajectory in both Figs. 7, 8 c). In order to estimate the trajectory of the bubble, we defined the bubble's center of gravity (x_c,y_c) and orientation as the central point of the bubble's projected image and the bubble orientation angle, θ shown in Figure 9 a). In each data we observed the trajectory of bubble. Figure 9 b) and c) show a histogram of the distribution of bubble trajectory in the y-direction; that is, distribution of y_c. We see from Fig. 9 b) and c) that while in stationary fluid (dark green bars) y_c is distributed near y/h=0.2, in shear flow (light green) the distribution lies beyond y/h>0.2. Especially for 16w% GWS shear flow, y_c is distributed from y/h =0.3 to 0.4. The fluctuation of the bubble trajectory toward span direction Δz was approximately $\Delta z/h$=0.07 in each condition. These results suggested that the shear rate acts on the ellipsoidal bubble as a lift force that induces bubble motion toward a direction where the relative velocity decreases (away from the belt). This general trend is the experiment conducted by Kariyasaki (1987). And it is also the opposite result to the small rigid sphere.

From Figs. 7, 8 and 9 we sought to reveal the correlation between the bubble's transverse movement and the bubble's orientation. Figure 10 shows the correlation between bubble orientation θ and bubble velocity in y direction (V_b). V_b at certain time t was calculated using equation (6) with the sampling rate Δt=23.5msec.

$$V_{b,t} = \frac{y_{c,t+\Delta t} - y_{c,t-\Delta t}}{2\Delta t} \qquad (6)$$

The figure shows a positive correlation between θ and V_b. The correlation function attained a high value,

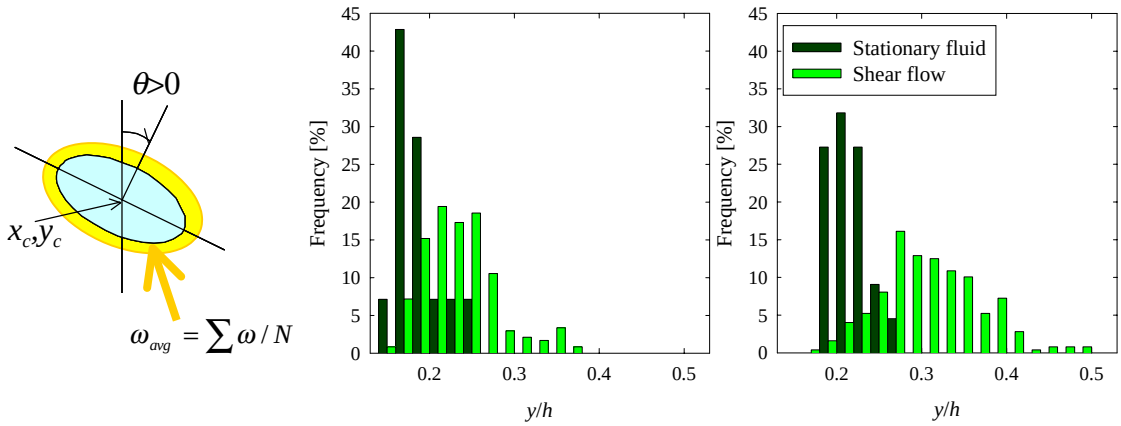

a) Definition of bubble parameters *b) In tap water* *c) In 16w%GWS*

Fig. 9. Trajectory of the bubble (distribution of y_c).

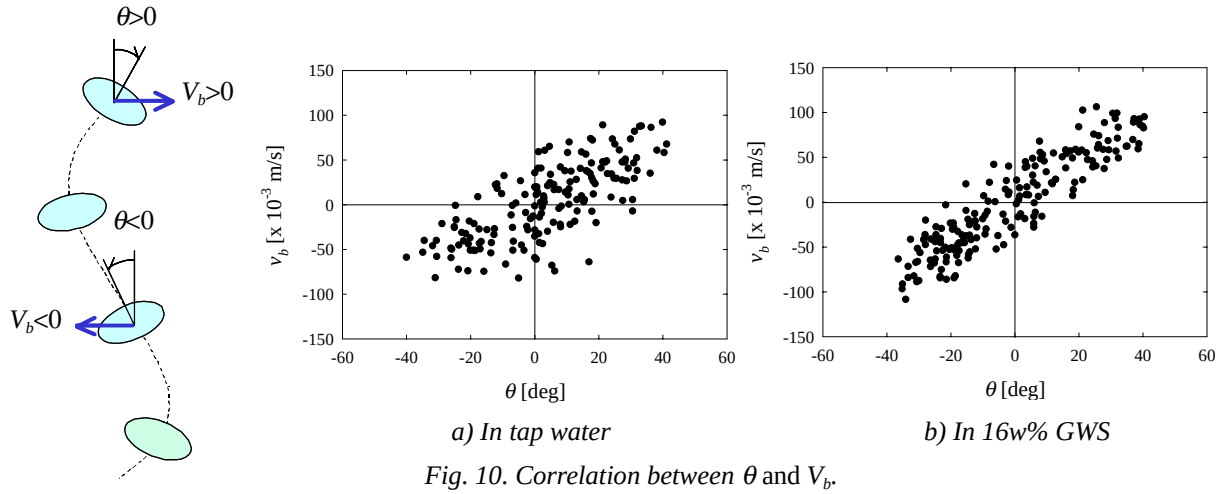

a) In tap water *b) In 16w% GWS*

Fig. 10. Correlation between θ and V_b.

$R_{\theta,Vb}$=0.73 in Figure 10 a) and $R_{\theta,Vb}$=0.91 in Figure 10 b). This figure suggested V_b and θ are related as schematically shown at the left. Figs. 7 and 8 suggest that the underlying mechanism revealed in Fig. 10 is the vortex shedding process.

To obtain the mechanism of the lift force on the bubble induced by the interaction of surrounding flow and bubble deformation shape more detail, we attempt to estimate the lift force using flow around the bubble and wake structure and we will testify the influence of the flow structure.

5. CONCLUSIONS

Using a DPIV/LIF/projection-technique, an experimental investigation on the flow structure in the vicinity of bubble in a vertical linear shear flow was conducted. We confirmed that the shear flow acts on the ellipsoidal bubble as a lift force, which induced bubble motion toward a direction where the relative velocity decreases. The underlying physical mechanisms of wobbly bubble motion is vortex shedding. The lift force on the bubble is influenced by the vorticity distribution in the wake of the bubble, especially at the edge of bubble where a vortex is shed. We quantitatively confirmed that the relative influence of vorticity, with respect to the trajectory of the bubble in the *y*-direction increases with shear rate *k*.

ACKNOWLEDGMENTS

This work was subsidized by the Grant-in-Aid of the Japanese Ministry of Education, Science and Culture (grant No. 11450088) and the Research Fellowships of the Japan Society for the Promotion of Science for Young Scientists (grant No. 03581).

REFERENCE

Brücker, Ch. (1998), “3-D measurement of bubble motion and wake structure in two-phase flows using scanning particle image velocimetry (3-D SPIV) and stereo-imaging”, 9th International Symposium on Applications of Laser Technique to Fluid Mechanics, pp. 27.4.1-27.4.10

Bunner, B. and Tryggvason, G. (1999), “Direct numerical simulations of three-dimensional bubbly flows”, Physics of Fluids, vol. 11, No. 8, pp. 1967-1969

Clift, R., Grace, J. R. and Weber, M. E. (1978), Bubbles, Drops, and Particles, Academic Press, New York (USA).

Fan, L.-S. and Tsuchiya, K. (1990), Bubble wake dynamics in liquids and liquid-solid suspensions, Butterworth-Heinemann Series in Chemical Engineering, Boston (USA)

Hao, Y. and Prosperetti, A. (1999), “The effect of viscosity on the spherical stability of oscillating gas bubbles”, Physics of Fluids, Vol. 11, No. 6, pp. 1309-1317

Kariyasaki, A. (1987), “Behavior of a single gas bubble in a liquid flow with a linear velocity profile”, Proceedings of the 1987 ASME-JSME Thermal Engineering Joint Conference, pp. 261-267. ASME, New York

Levich, V. G. (1962), Physicochemical Hydrodynamics, Prentice-Hall, Englewood Cliffs, New Jersey (USA)

Sakakibara, J., Hishida, K. and Maeda, M. (1993a), “Quantitative visualization of convective heat transfer near the stagnation region of an impinging jet”, Experimental Numerical Flow Visualization, ASME, FED-Vol. 172, pp. 93-99.

Sakakibara, J., Hishida, K. and Maeda, M. (1993b), “Measurement of thermally stratified pipe flow using image-processing techniques”, Experiments in Fluids, Vol. 16, pp. 82-96.

Tokuhiro, A., Maekawa, M., Iizuka, K., Hihsida, K., and Maeda, M. (1998), “Turbulent flow past a bubble and ellipsoid using shadow-image and PIV techniques”, International Journal of Multiphase Flow, 24, pp. 1383-1406

Tokuhiro, A., Fujiwara, A., Hihsida, K., and Maeda, M. (1999), “Measurement in the wake region of two bubbles in close proximity by combine shadow image and PIV techniques”, Transaction of ASME Journal of Fluid Engineering, Vol. 121, No. 1, pp. 191-197

Tomiyama, A. (1998), “Computational bubble dynamics”, Journal of the Japan Society of Simulation Technology, Vol. 17, No. 3, pp. 196-204